The Islamic University Journal (Series of Natural Studies and Engineering)
Vol.19, No.1, pp 57-70 , **2011**, ISSN 1726-6807, http://www.iugaza.edu.ps/ar/periodical/

Characteristics of left-handed multilayer slab waveguide structure

Mazen M. Abadla[1] and Sofyan A. Taya[2*]

[1]Physics Department, Alaqsa University, Gaza Strip, Palestinian Authority
Email: mazen@alaqsa.edu.ps
[2]Physics Department, Islamic University, Gaza, P.O.Box 108, Gaza Strip, Palestinian Authority. Email: staya@iugaza.edu.ps
*Corresponding author: Sofyan A. Taya, email: staya@iugaza.edu.ps

Abstract: We examine analytically the propagation of TE-polarized waves in a four-layer slab waveguide structure. One of the layers is considered as a Left-handed or metamaterial with simultaneously negative ε and μ. The dispersion relation of such a structure is shown in terms of the normalized thickness and the asymmetry factors. The effect of the doubly negative material parameters on the propagation characteristics has been examined. The variation of the effective index of the structure with different parameters of the layers is studied extensively. A comparison of the structure under consideration with the conventional right handed four-layer waveguide structure is also shown.

Keywords: Left-handed materials, slab waveguide, effective index, penetration depth.

خواص الموجهات الموجية المسطحة متعددة الطبقات المحتوية على مواد يسارية

الملخص: يدرس البحث انتشار الموجات المستقطبة عمودياً في الموجهات الموجيـــة المـــسطحة المكونة من أربع طبقات، إحدى هذه الطبقات مادة يسارية لها معامل سماحية ومعامل نفاذية سالبين، تم اشتقاق معادلة التشتت لهذه الموجهات ودراسة تأثير هذه المعـــاملات الـــسالبة علـــى انتـــشار الموجات، وكذلك تم دراسة تغير معامل الانكسار الفعال للتركيب المقترح مع المعاملات المختلفـــة مثل سمك الطبقة اليسارية وسمك الطبقة الموجهة، واهتم البحث كذلك بعقد المقارنات مع الموجهات الموجية المسطحة المألوفة المكونة من أربع طبقات.

1. Introduction

The process of development of integrated optics devices may comprise four steps. First, the function of the device is defined. Second, the architecture of the structure is determined. Third, a simulation process of the device is implemented. Fourth, the device fabrication and testing are examined. In this article we examine by simulation the properties of a four-layer slab waveguide structure which forms the actual components of active or passive devices.

Much progress has been made in the studies of multilayer optical waveguide due to its high importance as a basic guiding structure in integrated optics. Many applications have been proposed for the four-layer structure such as lens [1], large optical cavity laser [2], thin film taper coupler [3], and thin film waveguide TE-TM mode converters [4].

Recently, the concept of double-negative (negative ε and negative μ) materials has achieved remarkable importance due to the exhibition of unusual electromagnetic properties different from the known materials. These phenomena are observed in microwave, millimeter-wave, and optical frequency bands. The materials of double negativity are called metamaterials or Left-Handed Materials (LHMs). These are hand made structures that can be designed to exhibit specific phenomena not commonly found in nature. The LHM is a composite material in which both the electric permittivity ε and the magnetic permeability μ are simultaneously negative. The history of these materials begins with the work of Veselago [5], who proposed a medium with simultaneously negative ε and μ and studied the propagation of electromagnetic waves in such a medium. He predicted a number of unusual features of waves in LHMs, including negative index of refraction, the reversal of Doppler effect, and Poynting vector is antiparallel to phase velocity. Pendry et al [6] presented the artificial metallic construction of periodic rods which shows negative permittivity and they also presented a structure of split rings which exhibits a negative permittivity [7]. Smith et al [8] constructed a LHM using the combination of periodic rods and split rings and they performed many experiments in the microwave range to point out that the nature of this material is unlike any existing material. The first experimental investigation of negative index of refraction was achieved by Shelby et al in 2001 [9]. The interaction of electromagnetic waves with stratified isotropic LHMs was investigated by Kong [10]. He investigated the reflection and transmission beams, field solution of guided waves, and linear and dipole antennas in stratified structure of LHMs. The theory of LHMs and their electromagnetic properties, possible future applications, physical remarks, and intuitive justifications are provided by Engheta in 2003 [11]. Chew [12] analyzed the energy conservation property of a LHM and the realistic Sommerfeld problem of a point source over a LHM half space and a LHM slab. In 2006, Sabah et al [13] presented the reflected and transmitted powers due to the interaction of electromagnetic waves with a LHM. They studied the effects of the structure parameters, incidence angle, and the frequency on the reflected and transmitted powers for lossless LHM. The electromagnetic wave propagation through frequency-dispersive and lossy double-negative slab embedded between two different semi-infinite media was presented by Sabah et al [14]. Due to the fabrication technologies, the LHMs are widely used in filters, absorbers, lens, microwave components, and antennas, etc. Furthermore, many researchers continue to study the potential applications of LHMs [15-17].

In this article, we investigate analytically the propagation of electromagnetic waves in a multilayer waveguide structure. A lossless double negative slab is embedded between a semi-infinite substrate and a thin film as a guiding layer. The film is covered with a semi-infinite cladding. After examining the electric and magnetic fields using Helmholtz equation in the four layers, we study the wave penetration depth in the cladding and the substrate. The power in different layers is also derived. The effect of the doubly negative material parameters on the propagation characteristics has been examined. The variation of the effective index of the structure with different parameters of the layers is studied extensively. A comparison of the physical parameters of the proposed structure with that of the conventional right handed four-layer waveguide structure is also shown

2. Characteristic Equation

We consider the waveguide structure shown in Fig. 1. It consists of a guiding layer with permittivity ε_f, permeability μ_f and thickness d_3. The semi-infinite substrate has permittivity ε_s and permeability μ_s and the semi-infinite cladding has permittivity ε_c and permeability μ_c. An additional layer of Left-Handed material with negative permittivity ε_m, negative permeability μ_m and thickness d_2 is inserted between the substrate and the guiding layer. Here we assume all the materials are lossless. We also consider the TE waves in which the electric field ***E*** is polarized along the y-axis. Due to the symmetry between the electric and magnetic field ($\varepsilon \leftrightarrow \mu$, $E \leftrightarrow H$), the analysis of TM modes is similar to that of TE modes.

Waves are propagating along x-axis such that $E_y \sim e^{i\beta x}$, where β is propagation constant along x. Time harmonic fields have been assumed such that $E_y(x,z,t) = E_y(z)e^{i(b\,x - w\,t)}$. Due to the uniformity of the waveguide structure in y, the fields are uniform in y and Helhmholtz equation for the electric field reduced to an ordinary linear second order differential equation, namely,

$$\frac{d^2E_y(z)}{dz^2} + (k_0^2 e_i\, m_i - b^2)E_y(z) = 0,\ i \equiv s, m, f, c \tag{1}$$

The effective refractive index for the guiding mode N is defined as $\beta = k_0 N$, where $k_0 = w\sqrt{e_0 m_0}$. The wave equation becomes

$$\frac{d^2E_y(z)}{dz^2}+k_0^2(\varepsilon_i\,\mu_i-N^2)E_y(z)=0,\ i\equiv s,m,f,c \tag{2}$$

The waveguide structure under consideration supports a finite number of guided modes and an infinite number of unguided radiation modes. For guided mode solution, the power is required to be confined largely to the guiding layer (ε_f, μ_f). We here assume an oscillatory solution in the guiding layer such that $\varepsilon_f\ \mu_f - N^2 > 0$ and an evanescent tails in all other layers $\varepsilon_s\ \mu_s - N^2 < 0$, $\varepsilon_m\ \mu_m - N^2 < 0$, and $\varepsilon_c\ \mu_c - N^2 < 0$. The index of refraction of a given layer is $n_i^2=\varepsilon_i\mu_i$.

The solutions to Helmholtz equation for TE modes in the four layers are given by

$$E_{y1}(z)=Ae^{\gamma_s(z+d_2)},\ \ z<-d_2\ , \tag{3}$$

$$E_{y2}(z)=Be^{-\gamma_m z}+Ge^{\gamma_m z},\ \ -d_2<z<0 \tag{4}$$

$$E_{y3}(z)=C\cos(\gamma_f z)+D\sin(\gamma_f z),\ \ 0<z<d_3 \tag{5}$$

$$E_{y4}(z)=Fe^{-\gamma_c(z-d_3)},\ \ z>d_3 \tag{6}$$

where $\gamma_s=k_o\sqrt{N^2-\varepsilon_s\mu_s}$, $\gamma_m=k_o\sqrt{N^2-\varepsilon_m\mu_m}$, $\gamma_f=k_o\sqrt{\varepsilon_f\mu_f-N^2}$, $\gamma_c=k_o\sqrt{N^2-\varepsilon_c\mu_c}$, and the constants *A*, *B*, *C*, *D*, *F*, *G* represent the amplitudes of the wave in the layers.

It is convenient to express the characteristic equation of the optical waveguide in terms of the normalized parameters. Thus we begin by redefining the familiar normalized parameters commonly used in the three-layer case. We define a normalized thickness for layer 2 and layer 3 as

$$V_2=k_od_2\sqrt{\varepsilon_f\mu_f-\varepsilon_s\mu_s}\ ,\ \ V_3=k_od_3\sqrt{\varepsilon_f\mu_f-\varepsilon_s\mu_s} \tag{7}$$

Layers 1 and 4 have semi-infinite thicknesses and thus need not be normalized. We also define the asymmetry factor *a* and the normalized index *b* as

$$a=\frac{\varepsilon_s\mu_s-\varepsilon_c\mu_c}{\varepsilon_f\mu_f-\varepsilon_s\mu_s},\ \ b=\frac{N^2-\varepsilon_s\mu_s}{\varepsilon_f\mu_f-\varepsilon_s\mu_s} \tag{8}$$

In addition, we introduce a new parameter which can be called the guiding ratio [18].

$$\gamma=\frac{\varepsilon_m\mu_m-\varepsilon_s\mu_s}{\varepsilon_f\mu_f-\varepsilon_s\mu_s} \tag{9}$$

Characteristics of left-handed multilayer slab waveguide structure

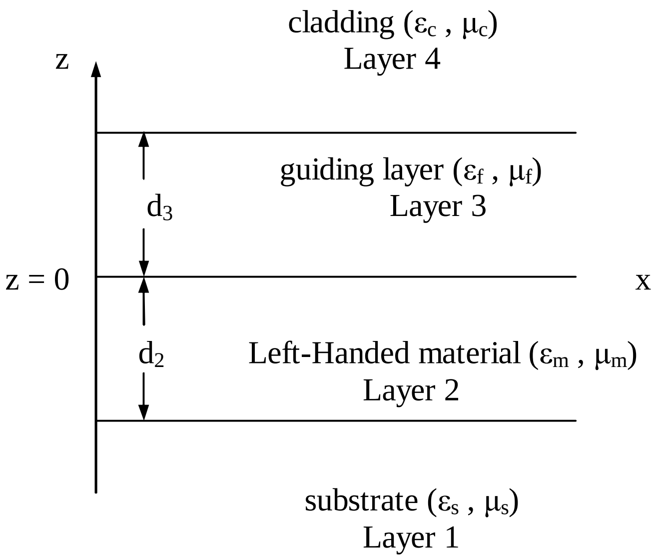

Fig. 1. Four-layer planar waveguide structure with layer 2 being left-handed material.

Matching the tangential components of the ***E*** and ***H*** fields, the characteristic equation of the structure shown in Fig. 1 can be written in terms of the above mentioned parameters as,

$$2V_3\sqrt{1-b} - f_{34} - f_{32} = 2mp \tag{10}$$

where f_{34} and f_{32} are the phase shifts at the boundaries above and below the principal guiding layer and are defined as

$$f_{34} = 2\tan^{-1}\left(\frac{m_f}{m_c}\sqrt{\frac{a+b}{1-b}}\right) \tag{11}$$

$$f_{32} = 2\tan^{-1}\left[\frac{m_f}{m_m}\sqrt{\frac{b-g}{1-b}}\,\frac{s_+ - s_- e^{-2V_2\sqrt{b-g}}}{s_+ + s_- e^{-2V_2\sqrt{b-g}}}\right] \tag{12}$$

where $s_+ = 1+\frac{m_m}{m_s}\sqrt{\frac{b}{b-g}}$ and $s_- = 1-\frac{m_m}{m_s}\sqrt{\frac{b}{b-g}}$.

3. Penetration Depth

The effective guide thickness is an important factor in the dispersion of the effective refractive index and in the application of optical sensing. Foreknowing this, we first calculate the effective guide thickness from the ray penetrations at the upper and lower boundaries of the guiding layer. The penetration of the guided wave from the guiding layer into the surrounding media can be written as [19]

$$x_2 = \frac{1}{2k_o N}\left(\frac{\partial f_{32}}{\partial g}\right) \tag{13}$$

$$x_4 = \frac{1}{2k_o N}\left(\frac{\partial f_{34}}{\partial g}\right) \tag{14}$$

where $N = \sqrt{e_f m_f}\,\sin(g)$ and g is the angle a ray makes with the normal to the boundary as shown in Fig. 2. In terms of the penetrations x_2 and x_4, the effective guide thickness is given by

$$d_{eff} = d_3 + x_2 + x_4 \tag{15}$$

and the normalized effective guide thickness can be written as

$$V_3' = k_o d_{eff}\sqrt{e_f m_f - e_s m_s} \tag{16}$$

Calculating the derivatives in Eqs. (13) and (14), we get

$$x_2 = \frac{m_f\sqrt{e_f m_f - N^2}\left(\sqrt{\frac{b-g}{1-b}}q_3 + q_2 s\right)}{m_m k_o N\left(1+\frac{m_f^2}{m_m^2}\frac{(b-g)}{(1-b)}s^2\right)} \tag{17}$$

$$x_4 = \frac{m_f(1+a)}{m_c k_o(1-b)\left(1+\frac{m_f^2}{m_c^2}\frac{(a+b)}{(1-b)}\right)\sqrt{N^2 - e_c m_c}} \tag{18}$$

where $s = \frac{s_1}{s_2}$, $s_1 = s_+ - s_- e^{-2V_2\sqrt{b-g}}$, $s_2 = s_+ + s_- e^{-2V_2\sqrt{b-g}}$,

$$q_2 = \sqrt{\frac{1-b}{b-g}}\frac{N(1-g)}{(1-b)^2(e_f m_f - e_s m_s)},\quad q_3 = \frac{-s_2(q+q_1) - s_1(q_1 - q)}{s_2^2},$$

$$q = \frac{m_m}{m_s}\sqrt{\frac{b-g}{b}}\frac{N\ g}{(b-g)^2(e_f m_f - e_s m_s)},\quad q_1 = e^{-2V_2\sqrt{b-g}}\left(q - \frac{2V_2 N s_-}{\sqrt{b-g}(e_f m_f - e_s m_s)}\right)$$

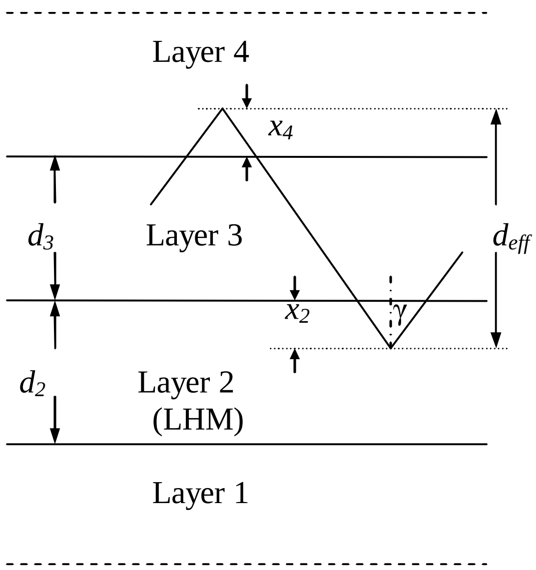

Fig. 2. Ray diagram illustrating the effective guide thickness d_{eff}.

4. Power flow through the waveguide layers

In this section we derive the power carried by each layer to fully investigate the four-layer waveguide properties when one of the layers is considered to exhibit a negative index of refraction. The guided wave power per unit length along x-axis is given by

$$P_{total} = \frac{Nk_o}{2wm} \int_{-\infty}^{\infty} E_y^2(z)dz \tag{19}$$

where ω is the angular frequency. Using Eqs. (3)-(6) to calculate the integral given by Eq. (19), we obtain

$$P_1 = \frac{Nk_o A^2 d_3}{4wm_s V_3 \sqrt{b}} \tag{20}$$

$$P_2 = \frac{Nk_o d_3}{4wm_m V_3 \sqrt{b-g}} \{-B^2(1-e^{2V_2\sqrt{b-g}}) + G^2(1-e^{-2V_2\sqrt{b-g}}) + 4BGV_2\sqrt{b-g} \tag{21}$$

$$P_3 = \frac{Nk_o d_3}{4wm_f V_3 \sqrt{1-b}} \{C^2 S_+ + D^2 S_- + CD[1-\cos(2V_3\sqrt{1-b})]\} \tag{22}$$

$$P_4 = \frac{Nk_o F^2 d_3}{4wm_c V_3 \sqrt{a+b}} \tag{23}$$

where $S_+ = V_3\sqrt{1-b} + \frac{1}{2}\sin(2V_3\sqrt{1-b})$ and $S_- = V_3\sqrt{1-b} - \frac{1}{2}\sin(2V_3\sqrt{1-b})$

When the continuity requirement is applied to Eqs. (3)-(6) and their derivatives, the following relations between the constants *A*, *B*, *C*, *D*, *F*, *G* are obtained

$$G = \frac{1}{2} A e^{V_2\sqrt{b-g}} \left(1 + \frac{m_m}{m_s}\sqrt{\frac{b}{b-g}}\right) \tag{24}$$

$$B = \frac{1}{2} A e^{-V_2\sqrt{b-g}} \left(1 - \frac{m_m}{m_s}\sqrt{\frac{b}{b-g}}\right) \tag{25}$$

$$C = B + G \tag{26}$$

$$D = \frac{m_f}{m_m}\sqrt{\frac{b-g}{1-b}}(-B+G) \tag{27}$$

$$F = C\cos(V_3\sqrt{1-b}) + D\sin(V_3\sqrt{1-b}) \tag{28}$$

5. Discussion

We have carried out the computations of the effective refractive index as a function of the guiding layer thickness (d_3), the thickness of the LHM layer (d_2) and the penetration depths (x_2 and x_4). In our calculations we suppose the cladding to have the lowest refractive index and the guiding layer to have the highest one, μ_m = -1 and λ = 630nm. Fig. 3 shows the variation of the effective refractive index with d_3. As d_3 approaches the cut-off thickness, the effective index approaches the substrate index n_s since in this limit all the power of the mode propagates in the substrate. The guided mode probes the substrate side only. As d_3 increases the confinement of the guided wave increases and the effective index approaches the guiding layer index n_f. For a given d_3, the effective index increases as n_f increases. Fig. 4 shows a comparison between the conventional four-layer waveguide with all the refractive indices being positive and the structure under consideration (i.e. Layer 2 is a LHM). It is clear that for a given d_3 and n_f, the conventional waveguide has a higher effective index. This behavior can be interpreted as: the evanescent wave generated at the boundary between the guiding layer and the LHM layer excites a surface wave at the boundary between the LHM layer and the substrate [20,21]. This effect enhances the field in the substrate so that the effective index decreases in the structure under consideration when compared with the case of four positive-index layers. The effective index as a function of layer 2 thickness d_2 (thickness of the LHM layer) is shown in Fig. 5. In contrary to its behavior with d_3, the effective index decreases with increasing d_2. Fig. 6 shows that the effective index decreases with increasing the penetration depths x_2 and x_4 and that it is very sensitive to the penetration depth x_4 in the cladding medium. This means that the structure under consideration is an eligible candidate for optical sensing applications.

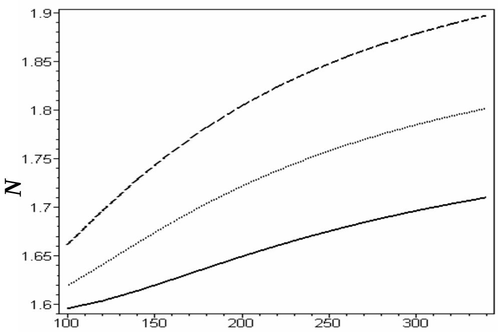

Fig. 3. Effective refractive index versus the guiding layer thickness for n_s = 1.55, n_c = 1.33, n_m = -1.65, d_2 = 100nm, n_f = 1.8 (solid line), n_f = 1.9 (dotted line), and n_f = 2 (dashed line).

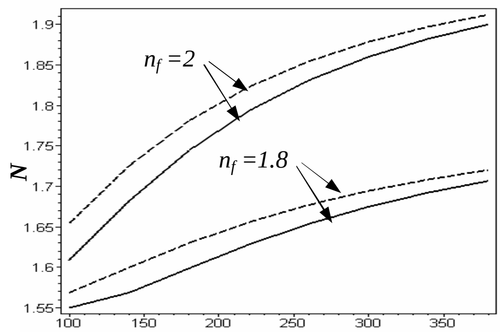

Fig. 4. Effective refractive index versus the guiding layer thickness for n_s = 1.55, n_c = 1.33, n_m = -1.65, d_2 = 100nm, for different values of n_f . The dashed lines represent the case when layer 2 is an ordinary dielectric with positive index and the solid lines represent the case when it is LHM.

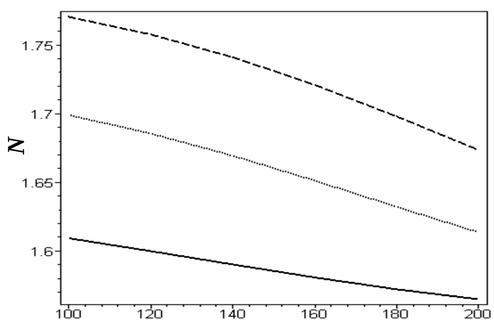

Fig. 5. Effective refractive index versus the thickness of layer 2 for n_s = 1.55, n_c = 1.33, n_m = -1.65, n_f = 2, d_3 = 100nm (solid line), d_3 = 150nm (dotted line), and d_3 = 200nm (dashed line).

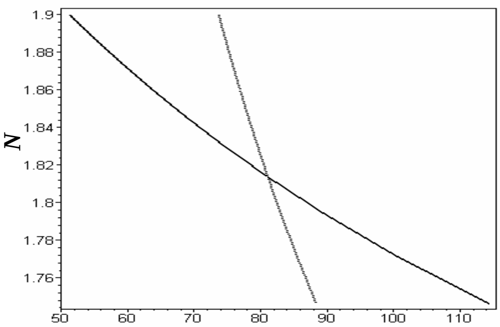

Fig. 6. Effective refractive index versus the penetration depths x_2 (solid line) and x_4 (dotted line) for n_s = 1.55, n_c = 1.33, n_m = -1.65, d_2 = 100nm, n_f = 1.8 and d_3 = 400nm.

The electric field configuration for the proposed structure is shown in Figs 7 and 8. As can be seen as the thickness of the LHM d_2 is increased from 50nm in Fig. 7 to 100nm in Fig. 8, two maxima arise in the field configuration. Thus the guided wave is supported by both of layer 2 and layer 3. Also we notice that the evanescent field strength in the cladding is higher in Fig. 8 (d_3 = 120nm) than that in Fig. 7 (d_3 = 100nm).

The powers P_2 in Layer 2, P_3 in the guiding layer, and P_4 in the cladding as functions of the thickness of the LHM layer (d_2) are shown in Fig. 9. As d_2 increases P_2 of the LHM increases while the power P_4 in the clad decreases. The power P_2 increases on expense of the cladding power. When the LHM layer thickness increases, the power concentrates in that layer because it becomes more bulky and nearly guiding. The powers P_1 in the substrate, P_2 in Layer 2, P_3 in the guiding layer, and P_4 in the cladding as functions of the guiding layer d_3 are shown in Figs. 10-13. For small values of d_3 (near cut-off thickness) most of the power flows in the substrate (P_1), and the powers P_2 and P_3 have minimum values. As d_3 increases, P_1 decreases and both P_2 and P_3 increase due to the guidance of the wave in these two layers. The power P_4 in the cladding has the minimum value among the other powers since the refractive index of this layer has the lowest value. To increase P_4 (power flow in cladding) for some applications such as optical sensing, a reverse asymmetry configuration is suggested. In this configuration, the index of the cladding is taken to be greater than that of the substrate. In this case, the part P_4 of the power increases and the part P_1 of the power decreases. Fig. 14 shows the fraction of total power flowing in the cladding as a function of the guiding layer refractive index n_f for different values of the refractive index of the LHM n_m. This fraction decreases with increasing the guiding layer refractive index due to the increase of the wave confinement in the guiding layer. For a given value of n_f, this fraction can be enhanced by increasing the absolute value of the refractive index of layer 2 (LHM).

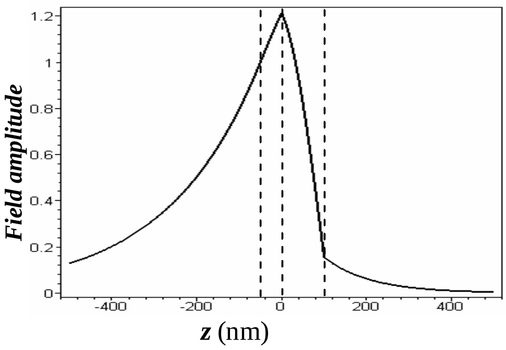

Fig. 7. Electric field configuration for n_s = 1.55, n_c = 1.33, n_m = -1.65, n_f = 2, d_2 = 50nm, and d_3 = 100nm.

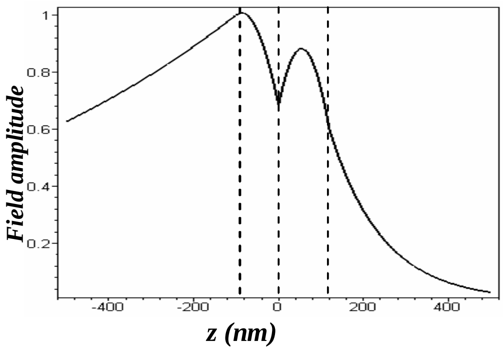

Fig. 8. Electric field configuration for n_s = 1.55, n_c = 1.33, n_m = -1.65, n_f = 2, d_2 = 100nm, and d_3 = 120nm.

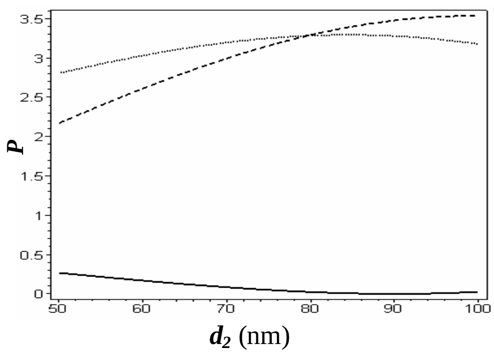

Fig. 9. Powers P_2 (dashed), P_3 (dotted), and P_4 (solid) versus the thickness of layer 2 for n_s = 1.55, n_c = 1.33, n_m = -1.82, n_f = 2, d_3 = 150nm.

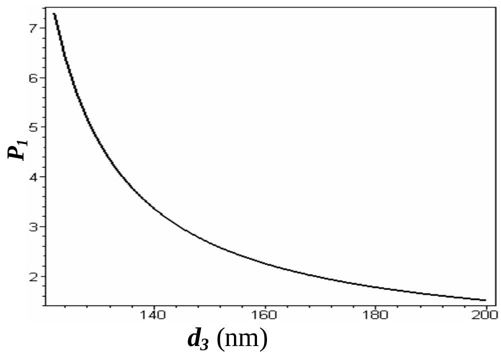

Fig. 10. Power flow in the substrate P_1 as a function of the guiding layer thickness for n_s = 1.55, n_c = 1.33, n_m = -1.82, d_2 = 100nm, and n_f = 2.

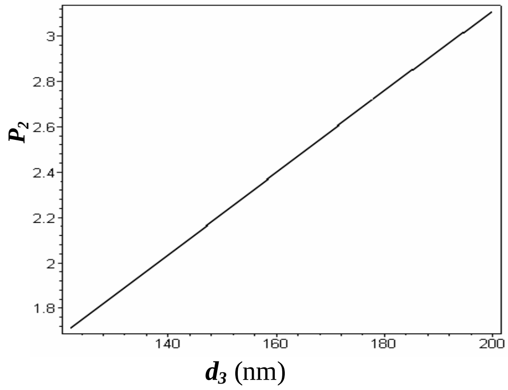

Fig. 11. Power flow in the layer 2 (LHM) P_2 as a function of the guiding layer thickness for n_s = 1.55, n_c = 1.33, n_m = -1.82, n_f = 2, and d_2 = 100nm.

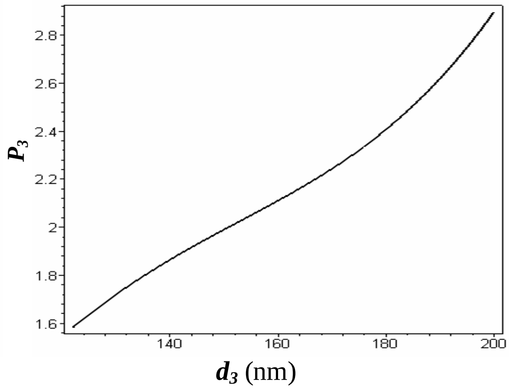

Fig. 12. Power flow in the guiding layer P_3 as a function of the guiding layer thickness for n_s = 1.55, n_c = 1.33, n_m = -1.82, n_f = 2, and d_2 = 100nm.

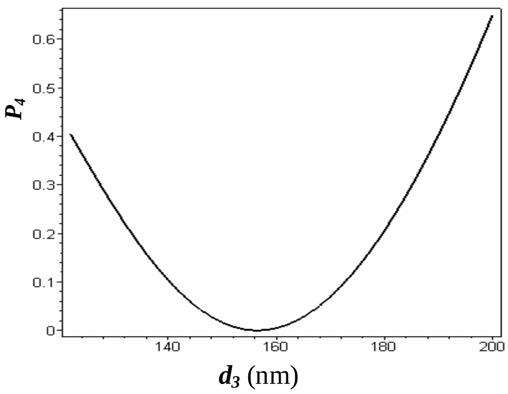

Fig. 13. Power flow in the cladding P_4 as a function of the guiding layer thickness for n_s = 1.55, n_c = 1.33, n_m = -1.82, n_f = 2, and d_2 = 100nm.

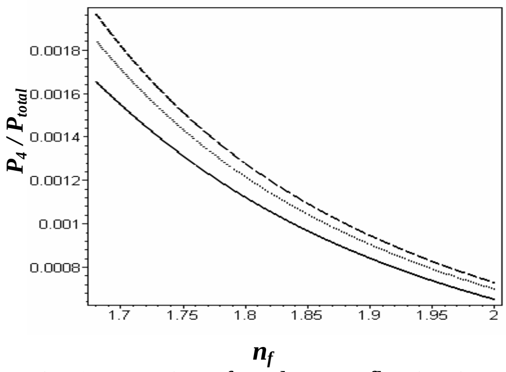

Fig. 14. Fraction of total power flowing in the cladding as a function of the guiding layer refractive index for n_s = 1.55, n_c = 1.33, n_m = -1.55 (solid line), n_m = -1.6 (dotted line), and n_m = -1.65 (dashed line).

6. Conclusion

In conclusion, we have analyzed a four-layer waveguide in which one of the layers is a left-handed material (LHM) of simultaneously negative ε and μ. The behavior of the effective refractive index with different parameters of the structure is studied and analyzed. The electric field configuration in such a structure is shown for different cases. The power flow in through the waveguide structure is also shown. We believe that structures containing LHMs can improve the performance of various slab waveguide devices.

References

[1] Southwell W., 1971- *Inhomogeneous optical waveguide lens analysis*, Journal Optics Society of America, Vol. **67**, p: 1004.

[2] Lockwood H., Kressel H., Sommers H., Hawrylo F., 1970- *An efficient large optical cavity injection laser*, Applied Physics Letters, Vol. **17**, p: 499.

[3] Tien P., Martin R., Smolinsky G., 1973- *Formation of light guiding interconnection in an integrated optical circuit by composite tapered-film coupling*, Applied Optics, Vol. **12**, p: 1909.

[4] Shibukawa A., Koba-yashi M., 1981- *Optical TE-TM mode conversion in double epitaxial garnet waveguide*, Applied Optics, Vol. **20**, p: 2444.

[5] Veselago V., 1968- *The electrodynamics of substance with simultaneously negative values of ε and μ*, Sov. Phy. Usp., Vol. **10**, p: 509.

[6] Pendry J., Holden A., Stewart W., Youngs I., 1996- *Extremely low frequency plasmons in metallic mesostructures*, Physical Review Letters, Vol. **76**, p: 4773.

[7] Pendry J., Holden A., Robbins D., Stewart W., 1999- *Magnetism from conductors and enhanced nonlinear phenomena*, IEEE Transactions on Microwave Theory and Techniques, Vol. **47**p: 2075.

[8] Smith D., Padilla W., Vier D., Nemat-Nasser S., Schults S., 2000- *Composite medium with simultaneously negative permeability and permittivity*, Physical Review Letters, Vol. **84**, p: 4184.

[9] Shelby R., Smith D., Schults S., 2001- *Experimental verification of a negative index of refraction*, Science **292**, 2001, pp. 77-79.

[10] Kong J., 2002- *Electromagnetic wave interaction with stratified negative isotropic media*, Progress in Electromagnetic research, Vol. **35**, p: 1-52.

[11] Engheta N., 2003- *Metamaterials with negative permittivity and permeability: background, salient features, and new trends*, IEEE MTT_S Int. Microwave Symp. Digest, Vol. **1**, p: 187.

[12] Chew W., 2005- *Some reflections on double negative materials*, Progress in Electromagnetic research **51**, p: 1.

[13] Sabah C., Ogucu G., Uckun S., 2006- *Reflected and transmitted powers of electromagnetic wave through a doubl-negative slab*, J. Optoelectronics and Advanced Materials **8**, p: 1925.

[14] Sabah C., Uckun S., 2007- *Electromagnetic wave propagation through frequency-dispersive and lossy double-negative slab*, Optoelectronics Review **15**, p: 133.

[15] Tretyakov S., 2001- *Meta-material with wide-band negative permittivity and permeability*, Microwave and Optical Technology Letters, Vol. **31**, p: 163.

[16] Caloz C., Chang C., Itoh T., 2001- *Full-wave verification of the fundamental properties of left-handed materials in waveguide configuration*, Journal of Applied Physics, Vol. **90**, p: 5483.

[17] Guven K., Ozbay E., 2006- *Near field imaging in microwave regime using double layer split-ring resonator based metamaterials*, Opto-Electron. Review, Vol. **14**, p: 213.

[18] Hewak D., Lit J., 1987- *Generalized dispersion properties of a four-layer thin-film waveguide*, Applied Optics, Vol. **26**, p: 833.

[19] Adams M., **An introduction to optical waveguides**, 1981, Wiley, Toronto.

[20] Ruppin R., 2000- *Surface polaritons of a left-handed medium*, Physics Letters A, Vol. **227**, p: 61.

[21] Qing D., Chen G., 2004- *Enhancement of evanescent waves in waveguides using metamaterials of negative permittivity and permeability*, Applied Physics Letters, Vol. **21**, p: 669.